Fracture of aircraft titanium alloys under high-frequency loading

Alexander D. Nikitin[1] · Pavel S. Shesterkin[1] · Sergey S. Lopatin[1]

Abstract

The paper is devoted to the problem of fatigue failure of two-phase titanium alloy VT3-1 under the action of high-frequency cyclic loading. Samples for the tests were made from the compressor disk of aviation engine D30-Ku installed on Tupolev Tu-154 planes. Repeated alternating loading was carried out by displacements of small amplitude at 20 kHz, coinciding with the first harmonic of longitudinal elastic vibrations of the sample. Analysis of specimen fracture surfaces shows predominant subsurface fracture. Analysis of areas of fatigue nucleation allows identifying elements of microstructure associated with crack nucleation. The results of the study can be used in the interpretation of fracture scenarios of structural elements in operation. Increasing the resource of products under such loads is possible through the use of damping layers or tapes, where possible.

Keywords Titanium alloy · Fatigue failure · Compressor disk · Microstructure · Crack initiation · Crack growth · Fracture surface

1 Introduction

The design and construction of complex technical systems is a set of aimed measures, among other things, at ensuring the reliability and safety of product operation. When designing aircraft components, one of the most important design parameters is also the requirement to reduce the weight of the product. As a rule, weight reduction and increase of product strength and reliability are not complementary [1–8]. Due to the difficulty of prediction, lack of exhaustive knowledge of physics and mechanics of cyclic failure and problems with estimation of fatigue strength of aircraft materials, it is fatigue failure of aircraft structure elements that is the dominant cause of unpredictable failure in operation. It is estimated that about 90% of the failure of aircraft elements in service is due to cyclic loading. The overwhelming majority of fatigue destructions in operation has a localized character and do not lead to a ship's death. The most widespread types of destruction are the tear-off of the gas-turbine engine blades, the destruction of the disk web, the destruction of auxiliary unit drive gears, the destruction of landing gear struts and the destruction of aircraft wing power elements, helicopter blades, etc. However, in the history of investigation of aircraft accidents, there are also many cases of fatigue failure. Among the most resonant ones we can mention the crash of Boeing 747 in Amsterdam (1992), when as a result of fatigue failure the third engine mounts failed, leading to separation of the power plant and consecutive collision with the fourth engine [9, 10]. As a result the airplane lost two engines on one wing and fell on the residential building. In modern practice, fundamental changes in loading modes and realized load spectra are observed. The experience of operating aviation and other transport equipment shows that the constant improvement of elements of power plant structures and the creation of new

✉ Alexander D. Nikitin, alexdnikitin@mail.ru; Sergey S. Lopatin, sergeyslopatin@mail.ru | [1]Moscow Aviation Institute, National Research University, Volokolamskoe Highway, 4, Moscow 125993, Russian Federation.

materials leads to the emergence of new modes of loading of structural materials, in which the existing methods of assessing the durability of products and diagnostics of failures associated with microdefects of their structure do not allow ensuring operational safety [7, 11–17]. One of such new loading modes is high-frequency cyclic loading with a frequency of about 1–3 kHz of blades and rim parts of gas turbine engine (GTE) compressor disks [18]. Such loading modes lead to the accumulation of a large number of load cycles (on the order of 10^8–10^{10} cycles).

Active research in the field of high fatigue life was started abroad in the mid-1990s with the allocation of a new section of knowledge about the fatigue behavior of materials: very high cycle fatigue (VHCF) [19]. The founder of the new direction of research was the French professor Claude Batia [20]. The separation of the field of VHCF into a separate direction of research is caused not only by the increase in cycles of loading, but also by a fundamental change in the mechanisms of microcrack nucleation. In contrast to the areas of low-cycle and high-cycle fatigue (LCF 10^3–10^5 cycles and HCF 10^5–10^7 cycles), where nucleation occurs from the surface of the sample and is associated with the formation of slip bands, in the field of VHCF, cracks are nucleated in the internal volumes of the material, which is caused by processes of microplastic deformation accumulation in the neighborhood of microstructure heterogeneities (inclusions, pores, grain boundaries, etc.) [21, 22]. For a long time, the study of VHCF region has been difficult due to the unacceptably long duration of tests to achieve the ultimate durability of specimens. However, with the invention of fundamentally new loading devices with a loading frequency of ~ 20 kHz [23], based on resonance principles and the piezoelectric effect, it became possible to conduct representative studies in a reasonable time frame (24–49 h to achieve 10^9 cycles).

After the first international conference on VHCF-1 in 1998 in Paris by Professor Claude Batia, interest in VHCF research began to increase dramatically. As the experimental base accumulated, it became clear that different materials, although they have different resistance to resonant cyclic loading in the field of VHCF, but there is no "fatigue limit" defined by the test standards for them [23]. For some structural materials, such as steels, titanium alloys, etc., the difference between fatigue limits determined on the basis of 10^7 and 10^9 cycles can reach up to 40%. Due to such behavior of structural materials in the field of VHCF [24], the estimation of safe service life of products made of them by traditional methods may not be correct, which may eventually lead to unpredictable failures of products in service [6, 8, 11]. Studies of the fatigue behavior of titanium alloys in VHCF region [25–27] also showed a significant decrease in fatigue strength in VHCF region with the allocation of an additional branch of the fatigue curve

characterized by subsurface fatigue crack initiation. The presence of a bimodal fatigue life distribution contributed to the development of the fatigue life estimation model in VHCF region as a generalized multiaxial criterion [28, 29]. A study of this branch for the titanium alloy VT3-1 [30] showed a qualitative dependence of the fatigue life of the material on the type of microstructure defect that led to crack initiation. Currently, there are no models and criteria to quantify the relation between geometry and defect type and fatigue life. Currently, an approximate model by Yakitoki Murakami [31] is used to estimate the fatigue life of structural materials by the area of the maximum defect cross section characteristic of the material. In this case, the assumption is made that failure should occur exactly along the maximum defect cross-section, which is not always true in conditions of complex multiaxial stress state for real structural elements. For Russian structural materials, studies in the field of VHCF have been carried out to a limited extent and mainly for titanium alloys [32–38].

Despite the small number of experimental data, the importance of research in this area is due to the increasingly frequent failure of critical structural elements with obvious traces of high-frequency fracture. The Fig. 1 shows a two-phase titanium alloy disk destroyed in operation after a 30% service life. Thus, this failure is considered as an early and unpredicted failure. Analysis of fracture surface of the disk and blade's mating part showed that fatigue crack initiation occurred at insignificant distance from the surface. A facet corresponding in morphology to the alpha phase grain of the material was found in the fatigue fracture zone.

The fracture bears the traces of quasi-brittle splitting of the alpha phase. Studies of the chemical composition in local zones with a capture of 1 μm showed chemical heterogeneity in the specified zone. Integral evaluation of the chemical composition within tens of micrometers showed full compliance of the material with the state standards. Thus, this peculiarity of fracture cannot be associated with a violation of the technological process and is associated primarily with loading conditions. According to the above data for foreign titanium alloys, such fatigue behavior is associated with high-frequency fatigue loading. In the present work the behavior of Russian two-phase titanium alloy under high-frequency cyclic loading is investigated.

2 Materials and methods

Fatigue tests of titanium alloy VT3-1 were carried out on a piezoelectric device LASUR [22, 39], which allows loading with constant amplitude of displacements in the resonant mode. The principles of piezoelectric fatigue tests were proposed by Manson in 1950th [40] and later developed

Fig. 1 Appearance of the destroyed titanium disk of Tupolev Tu-204 aircraft (**a**) and fracture surface of the destroyed blade (**b**) [8, 9]

(a)   (b)
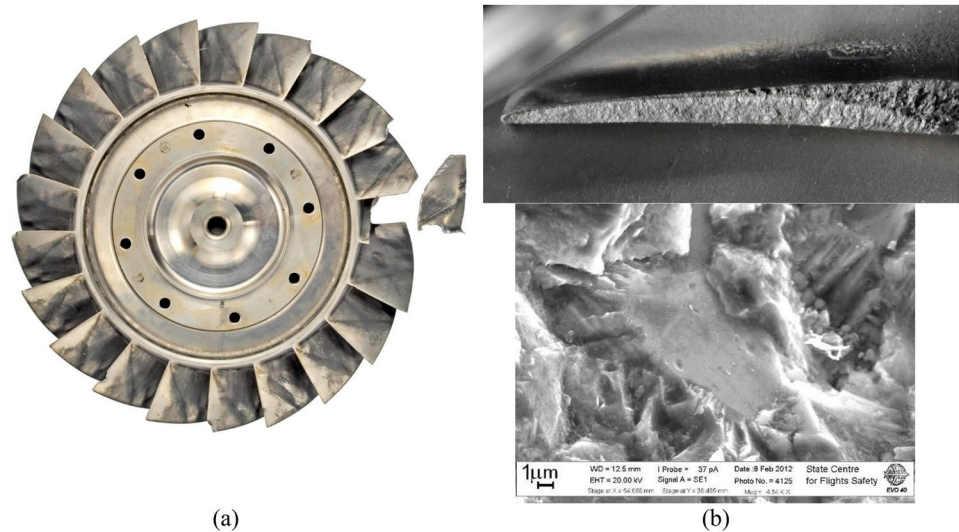
by Prof. Claude Bathias. Based on developed by Prof. C. Bathias patent a set of piezoelectric system were installed including the LASUR, SHIMADZU USF-2000A and some modern systems. Several ASTM standards on ultrasonic fatigue testing methods were developed by Prof. Bathias with co-authors [41]. The ultrasonic fatigue testing LASUR allows a high accuracy control of loading parameters (frequency and amplitude) with effective electronic feedback. The control unit allows the constant amplitude loading with maximum error less than 1 μm. The external view of the loading device is shown in the Fig. 2 (a). The piezoelectric device consists of a control unit, including a personal computer with an integrated high-performance card, which exchanges and converts data with the executing mechanisms at high speed and a block of executing devices. The executing or loading devices include oscillator, piezoelectric converter, booster and waveguide. All mechanical connections of these elements are made by means of internal screw connections. The contact surfaces are treated with silicone lubricants against wear of the contact surfaces. Test specimens are connected to the waveguide by means of M5 screw (internal connection). It is possible to realize a loading scheme with different

coefficients of cycle asymmetry. In case of realization of symmetric loading cycle ($R = -1$), one waveguide can be used with specimen attachment, presented in the Fig. 2 (b).

For tests with positive cycle asymmetry ($R > 0$), two symmetrical waveguides can be used, as it is shown in the Fig. 2 (a). The tests were carried out in air at room temperature. Cooled compressed air, supplied at a pressure of 2 atmospheres, was used to provide cooling of the working part of the sample. A contact method using strain gauges was used to ensure calibration of the system. The calibration of the system allows the relation between the applied displacements to the end of the specimen and the deformations in the working part. Due to tests in the elastic behavior of the material, the deformations are unambiguously converted into stresses by means of the dynamic modulus of elasticity.

The principle of resonant loading tests is that displacements are applied at one end of the specimen at a frequency that coincides with the resonant frequency of the specimen. The principal feature of such loading is to control the test process by controlling the displacement amplitude. It is known that in the case of resonant

Fig. 2 Exterior view of VHCF testing machine (**a**) and elements of the sample calibration system (**b**)

(a)   (b)
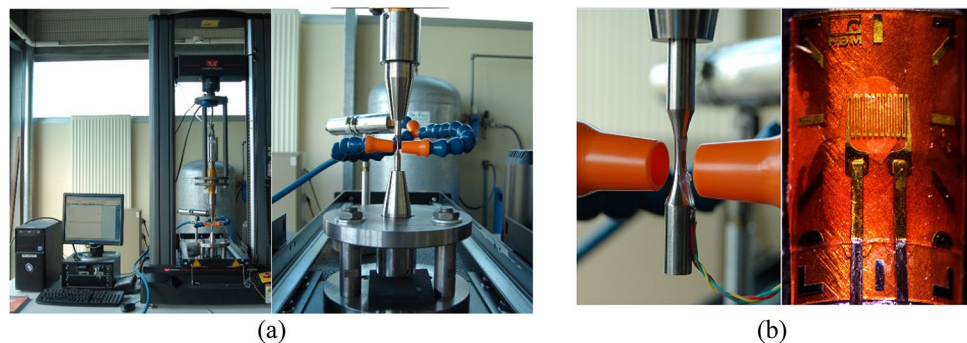
loading, when the frequency of external loading coincides with the natural frequency of vibration of the product, the amplitude of the loads increases indefinitely and is determined by the coefficient of dynamism of the structure. This statement is true for the case of force loading, when the displacement amplitude grows indefinitely. In the case of VHCF tests, the loading parameter is the displacement amplitude, which is a set and controlled by a personal computer throughout the entire period of testing the specimen. Thus, the tests are conducted in resonance mode, but the stress amplitudes do not tend to infinity, but are determined by displacement amplitudes and damping coefficients for a given material.

Based on the above, it becomes obvious that the development of the geometry of VHCF specimens for testing various materials becomes a scientific and research task. To ensure standardization of tests, the following scheme of geometry development is used: the central cross-section of specimens remains unchanged for any type of materials (Fig. 3), while the selection of natural frequency in the vicinity of 20 kHz for the specimen is performed by changing the length of the cylindrical part of the specimen. This length is often referred to as "resonance length".

To manufacture the samples from titanium alloy VT-3, compressor disk of D30-Ku engine was used (Fig. 3 (a)). Blanks for the samples were obtained by electroerosion method from the rim part of the disk in the form of cylinders with a diameter of 12 mm. Then, from the blanks were made corset specimens shown in the Fig. 3 (b) with a diameter of 10 mm and a working part of 3 mm. After fabrication, the surface of the specimens was mechanically polished to eliminate residual stresses and surface machining defects.

The microstructure of the titanium alloy was examined in three mutually perpendicular directions (Fig. 4) by optical microscopy Olympus MX63. The microstructure analysis shows a classical lamellar structure without obvious features. Careful analysis of the microstructure reveals some zones with an ordered arrangement of alpha plates within it. It is also possible to detect traces of texturization arising in the process of stamping the material. In general, the morphology of microstructural elements is homogeneous, without inclusions and represented by elongated alpha-plates with a characteristic length of 10–15 microns and a width of a few microns. Details of the structural structure of the alloy are shown in the Fig. 4 (b). Beta phase

Fig. 3 Titanium disk of D30-Ku engine compressor (a) and specimens for uniaxial VHCF tests (b)
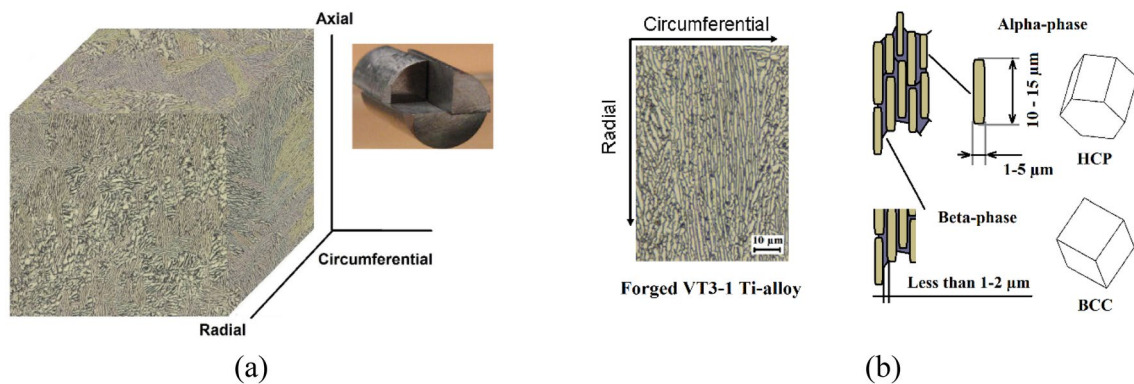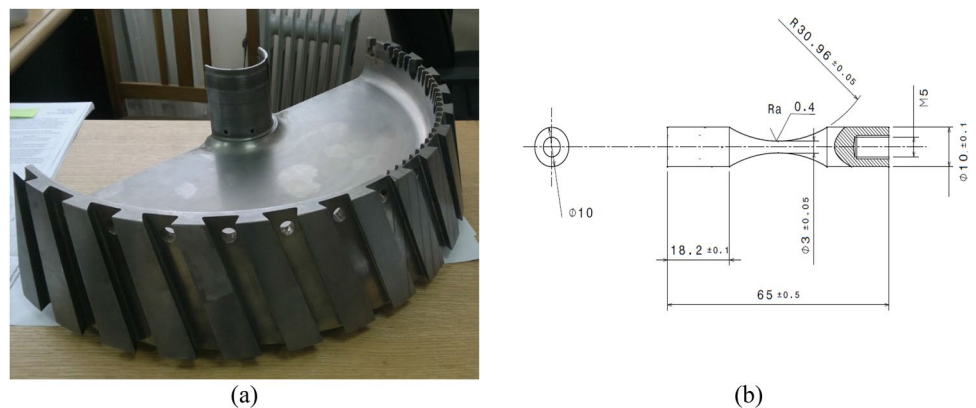

Fig. 4 Microstructure of titanium alloy VT3-1 in three mutually perpendicular planes (a) and schematic representation of microstructural elements (b)

is distinguished at the boundaries of alpha-plates. In the Fig. 4 it is presented by darker color.

The chemical composition and mechanical properties of the alloy do not differ from the values recommended in the state standard. The composition was evaluated by using EDX module of Carl Zeiss EVO 40 scanning electron microscopy. When analyzing the thin film on the energy dispersion unit within the zone of 30 microns by 80 microns, the integral assessment showed the presence of all the necessary alloying elements within the permissible values: aluminum: 6.1%, molybdenum: 2.7%, chromium: 1.6%, iron: 0.5%. No peculiarities in the form of non-metallic inclusions were detected. Tests of mechanical properties were carried out on standard samples by using INSTRON 5969 tensile machine and showed the following results: tensile strength: 989 MPa, yield strength: 960 MPa, longitudinal deformation at break: 6%, dynamic Young's modulus: 114 GPa.

3 Results and discussion

Fatigue tests were conducted in air under normal conditions. A stepwise loading with a step between adjacent levels of 15 MPa was chosen as the test method. The number of tested specimens is following tensile-compression tests with $R = -1$ is 21 specimens (7 specimens of S-set, 7 specimens of M-set and 7 specimens of L-set); the fully reversed torsion tests is 5 specimens. The difference between sets was in resonant length. Since the mechanical properties of forged material could have some variation due to texture the specimens were machined with small increment in resonance length (0.5 mm). The torsion tests were performed on the in-house developed piezoelectric fatigue torsion system [42] and are the only VHCF torsion test results in the World on a titanium alloy. Tests were performed on the basis of 10^9 cycles with an automatic crack detection algorithm. When a fatigue crack is present in a structure, its stiffness decreases, resulting in a decrease in the resonant frequency. As soon as the resonant frequency of the test goes beyond the allowable range, the test is stopped. As a result of tests, fatigue curves were obtained for alloy VT3-1 under different types of loading: tension–compression (Fig. 5 a) and torsion (Fig. 5 b). The results of torsion tests were recalculated into equivalent stresses by using equivalent Von Misses stress $\sigma_{eq} = \sqrt{3} \cdot \tau_a$ (τ_a is an amplitude of torsion load) for comparison with the results of uniaxial tests. As we can see from the presented fatigue curves, the titanium alloy VT3-1 shows no physical limit of fatigue in the area of high durability. The Fig. 5 show the results for broken and run our specimens. Also, the indication of surface and subsurface crack initiation is provided. The Fig. 5 b show the result for only broken tension–compression specimens since all the torsion specimens were failure. There are no run out results for torsion tests. There is no clear horizontal asymptote for uniaxial loading and for the case of torsional vibrations. The confidence interval of the experimental data is following (1) for tension compression $R = -1$ tests is 12.7 MPa, for fully reversed torsion is 5.1 MPa.

Titanium alloy exhibits sensitivity to the type of loading. In torsion, for example, the slope of the fatigue curve is steeper than in compression tensile. In both cases, fracture occurs in the range of 10^7 to 10^9 cycles, which exceeds standard test bases for this class of material. According to generally accepted test standards, two-phase titanium alloys belong to the "physical fatigue limit" group of materials, which allows their fatigue
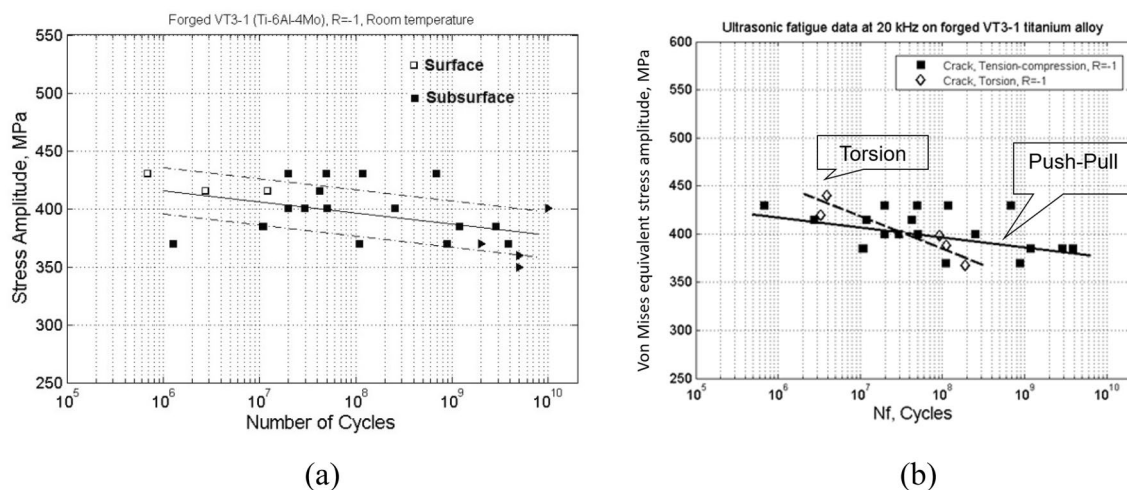

Fig. 5 Results of fatigue tests of titanium alloy VT3-1

strength to be evaluated on the order of $2 \cdot 10^6$ cycles [43]. Nevertheless, experimental data indicate that such materials can fail at high operating times at stress levels well below the classical cyclic strength limits, which creates additional risks of unpredictable failure of elements of aircraft structures cut from such materials and subjected to cyclic loading.

Analysis of the fracture surface for such materials shows that the decrease in cyclic strength in the range of high durability is also accompanied by a change in the mechanism of fatigue crack nucleation. Thus, when the material works in the field of multicyclic fatigue, the characteristic mechanism of fracture is the formation of a single surface crack and its subsequent growth. In the case of loading in the area of high durability or in the area of VHCF, subsurface nucleation of fatigue cracks with formation of foci in the vicinity of microstructural defects prevails. Nevertheless, surface nucleation is also observed, although the fraction of such fractures is much lower. The Fig. 6 shows the results of fractographic analysis of a typical fracture surface of VT3-1 titanium alloy in the region of VHCF at surface and subsurface nucleation. In the Fig. 6 the arrows indicate the areas of fatigue cracks nucleation. With surface nucleation, two different types can be distinguished: crack nucleation with the formation of stress concentrator and subsurface nucleation from the existing concentrator in the form of agglomeration of elements with high microhardness. In the case of concentrator formation, the mechanism of fatigue crack nucleation is similar to that of multicyclic fatigue. In the basic variant, the formation of plastic deformation traces in the form of sliding bands takes place. In the process of cyclic fatigue, slip bands develop with the formation of extrusions and intrusions, the destruction of individual alpha plates, their "splitting" and the formation of a stress concentrator in the form

of surface microcracks. In the case of an existing defect, the homogeneity of the stress–strain state in the vicinity of the feature is violated due to the different deformation abilities of the material.

The deformation at a local zone is being quasi the same with some deviation at the microscale level. The higher local stress under the same deformation will be observed in the volumes with higher elastic moduli. In the case of two-phases titanium alloy the coarse alpha-grains experience higher local stress compared to surrounded matrix. Moreover, the microhardness measurements show higher value for coarse alpha-grains that means a lower plasticity. In this case a hard volume with the lower possibility for plastic deformation is cycling under a given tensile deformation. Such loading conditions together with coarse grain deformation behavior led to "quasi-brittle" failure As a result, the material of the feature in the form of an agglomeration or cluster of alpha plates experiences higher local stresses than the basic material and active degradation of the feature occurs. This process results in "quasi-brittle" failure of the peculiarity (Fig. 7) and formation of a stress concentrate in the form of a crack.

The Fig. 7 shows a near-surface fracture with subsequent growth of a fatigue crack into the volume of the material. A similar scenario of crack development is indicated by the practical circular shape of the crack front at the apex of the microstructural feature. After reaching the crack surface, the morphology of the fracture surface changes, with a prominent stitching indicating a change in the crack growth rate.

In the case of subsurface nucleation of fatigue cracks (Fig. 8) we can also distinguish two fundamental differences in the scenario of damage development. One scenario is associated with the presence of microstructural features in the form of extended macrozones, agglomerations of hard structures, heat treatment features, etc., and the second scenario is associated with the basic

Fig. 6 Characteristic fracture surface of the specimen made of VT3-1 titanium alloy in the region of VHCF with **a** surface and **b** subsurface nucleation
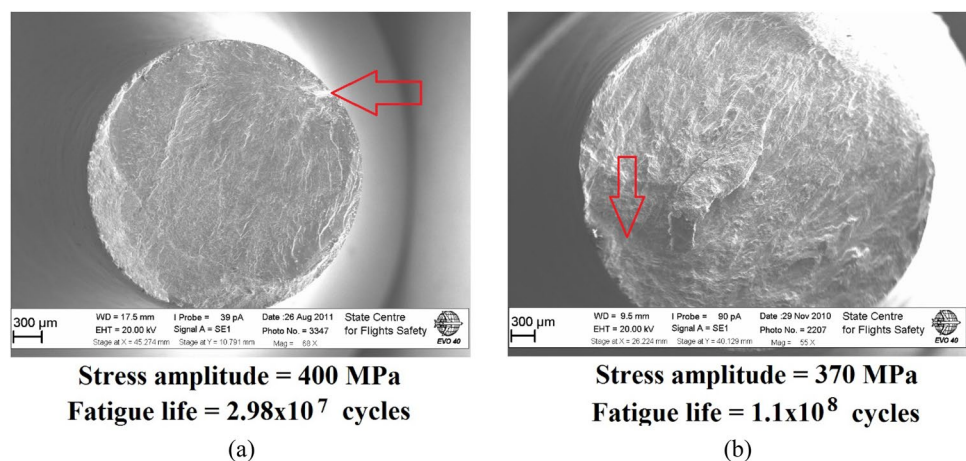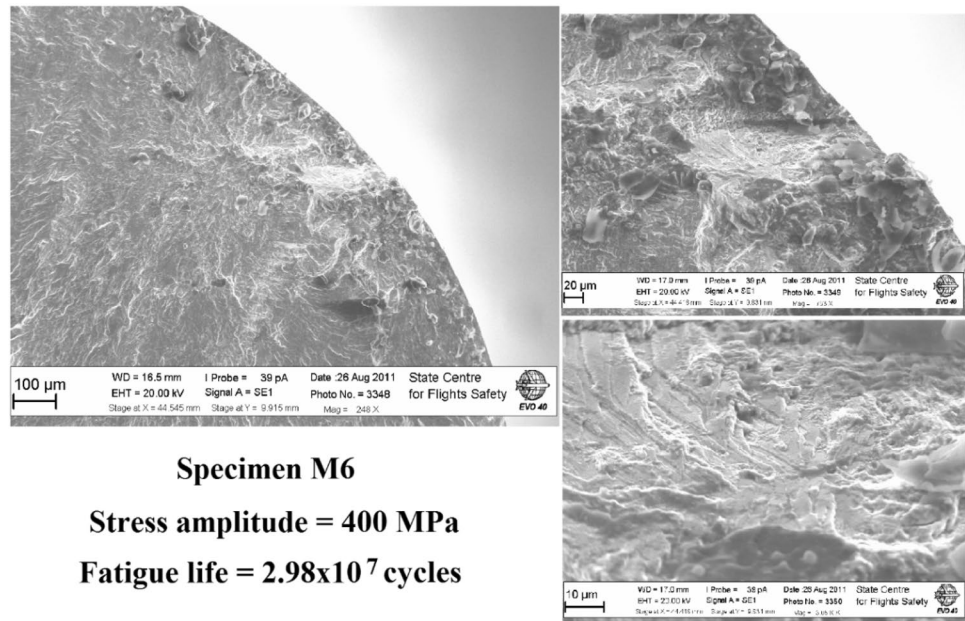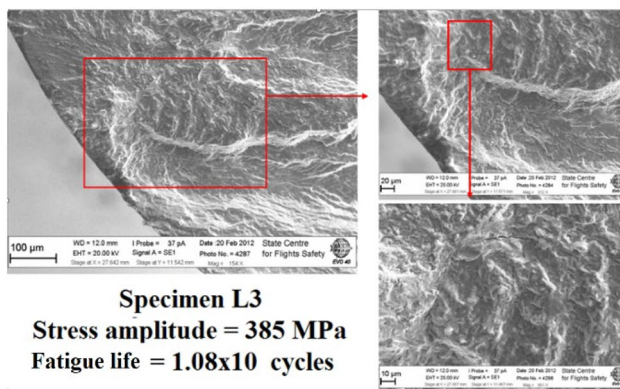

Stress amplitude = 400 MPa
Fatigue life = 2.98×10^7 cycles
(a)

Stress amplitude = 370 MPa
Fatigue life = 1.1×10^8 cycles
(b)

Fig. 7 Fracture of titanium alloy VT3-1 in VHCF region as a result of quasi-brittle fracture of alpha plate agglomeration
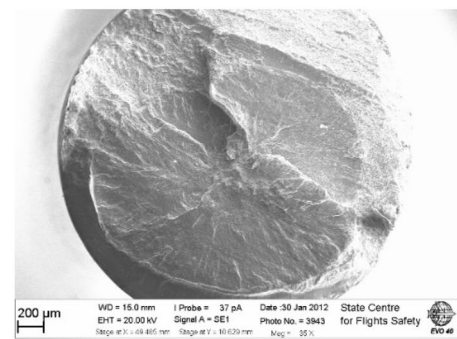

Fig. 8 Examples of subsurface initiation of a fatigue crack in titanium alloy VT3-1 from an existing microstructure defect in the form of macrozone boundary (**a**) and from a formed concentrator in the form of smooth facet (**b**)

properties of the alloy and the formation of a stress concentrate in a regular structure without features.

In the case of subsurface nucleation of a fatigue crack from the macrozone boundary, fracture may be associated with the accumulation of dislocations at the boundary of an extended microstructural object. The microhardness in such areas is usually lower than the average value (Fig. 9a) for the material, which indicates a facilitated plastic deformation in these areas. This is achieved due to the fact that the structural elements in the form of alpha phase plates are oriented in the same way within a large volume. Dislocation displacement in this case meets little resistance at the boundaries of

such microstructural elements and allows large runs to be realized.

Significant obstacles to the movement of dislocations arise at the boundaries of macrozones, since neighboring regions may have different crystallographic orientations (Fig. 9 b). In this case, microscopic plastic deformation begins to form at the boundary of such extended macrozones, leading to changes in the loyal stress fields. Accumulation of microplastic deformation requires a sufficient number of loading cycles, so it does not always have time to manifest itself, especially if the material has significant surface defects or a serious violation of the microstructural structure.
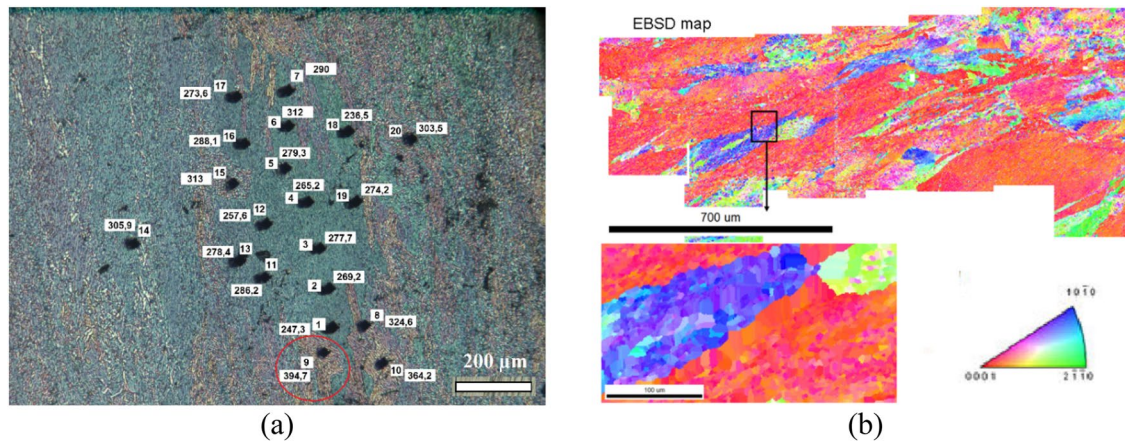
Fig. 9 Examples of microhardness measurements of VT3-1 titanium alloy in the macrozone (**a**) and example of electron backscatter diffraction (EBSD) analysis of a significant surface of a thin section (**b**)

In case of regular nucleation of fatigue crack in two-phase titanium alloy the focus is formed as a smooth facet (Fig. 10 a). This type of nucleation is caused by destruction of individual plates of alpha phase of titanium alloy. Analysis of chemical elements distribution (Fig. 10 b), within such facets tells about essential redistribution of chemical elements in local zone. Thus, a high concentration of aluminum is observed in the body of the alpha plate, exceeding the maximum standard value by almost 30%. The minimum permissible value in such areas exceeded twice. Thus, the presence of significant redistribution of chemical elements changes the mechanical properties and microhardness of local material volumes. The presence of components with different deformation properties leads to the formation of local stress concentrations and fatigue

degradation of the material. This fracture mechanism in VHCF region is common to all two-phase titanium alloys regardless of chemical composition. Numerous results of fatigue tests on Ti-6Al-4 V show that this mechanism is dominant for this alloy [44–47].

The process of formation of such a concentrator is the most time-consuming in comparison with nucleation from microstructure features in the form of macrozones or alpha plate agglomerations. There are many models and explanation on how and why such structures are forming [44–48]. The analysis and study of this feature of fatigue crack initiation in titanium alloy should be provide in the independent article. In the framework of present study, we may only indicate that most likely, the formation of the first facet is caused by the following factors: (1) crystallographic
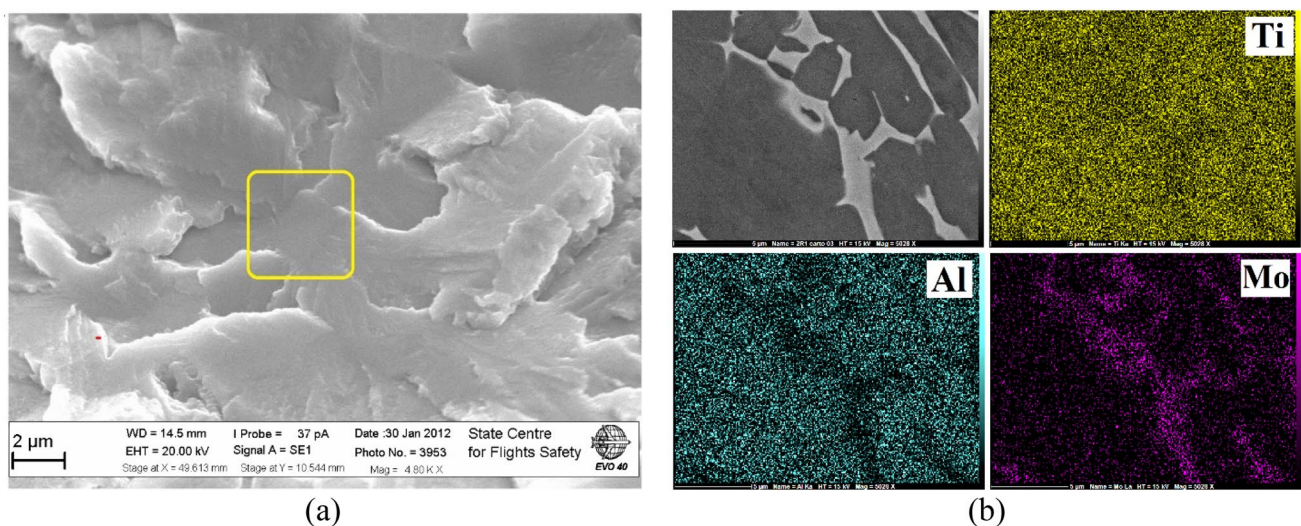

Fig. 10 Area of fatigue crack nucleation during formation of a hearth under the surface in the form of a smooth facet (**a**) and an example of chemical elements mapping in a similar area (**b**)

orientation of the facet relative to the axis of loading, (2) crystallography and morphology of the surrounding facets and (3) local stress field in the vicinity of the facet. Subtle studies of fracture surfaces have shown that different slip planes are activated depending on the location of the facet at the surface or in the volume of the material. Thus, the position and the local stress field determine the slip system (pyramidal or basal) in which the predominant slip of dislocations occurs. The crystallographic orientation of neighboring facets determines the rate of dislocation accumulation at facet boundaries. In the case of a serious barrier preventing dislocations from passing from one facet to another, the process of microplastic deflocculation accumulation will be more pronounced compared to the case of partial dislocation movement into neighboring alpha-plates. The accumulation of dislocations on the facets can also be influenced by the interface conditions. The analysis of fracture surfaces of VT3-1 titanium alloy makes it possible to distinguish characteristic features of fracture morphology testifying to the presence of high-frequency loading. The main ones among them are subsurface nucleation and the presence of smooth facets with traces of quasi-brittle fracture.

4 Conclusions

The study of two-phase aviation titanium alloy VT3-1 under high-frequency resonant loading has been carried out. It is shown that for two-phases titanium alloy alloys there is no "physical" fatigue limit in the region of high durability. Fatigue curves show a continuous decrease in cyclic strength. It is found that fatigue characteristics of two-phase titanium alloy have sensitivity to the type of stress–strain state in the region of long durability. Torsional fatigue resistance is found to be lower than under uniaxial loading due to the fact that curves for two loading conditions intersect. The pure torsional fatigue curve in VHCF region has a larger slope angle. Microscopic studies of fracture surfaces show a fundamental change in the mechanism of crack nucleation and growth under VHCF loading. It is shown that the transition to subsurface fracture occurs when the material fractures under cyclic loads below the fatigue limit. Subsurface fracture becomes dominant after over 10^8 cycles. Thus, methodological recommendations for interpretation of fracture surface morphology of aviation products in operation are formed. Presence of subsurface fracture with formation of smooth facets may indicate presence of high-frequency component of loading, leading to fast cycles' operating time. Besides, analysis of fracture surfaces of specimens with subsurface nucleation has allowed revealing characteristic features of microstructure, such as large agglomerations of alpha phase and borders

of extended macro zones leading to premature fracture in the region of VHCF. The formation of facets with traces of quasi-brittle fracture was established as the basic mechanism. This type of destruction is caused by the distribution of chemical elements during crystallization, crystallographic orientation and parameters of neighboring alpha plates.

Declarations

References

1. Wanhill RJH, Oldersma A (1997) Fatigue and fracture in an aircraft engine pylon. National Aerospace Laboratory NLR, Amsterdam
2. Beynon JH, Brown MW, Lindley TC, Smith RA, Tomkins B (1999) In: Balkema AA (eds) Rotterdam engineering against fatigue. Springer London pp 1–10
3. Pronina PF, Sun Y, Tushavina OV (2020) Mathematical modelling of high-intensity heat flux on the elements of heat-shielding composite materials of a spacecraft. J of Appl Eng Sci 18(4):693–698. https://doi.org/10.5937/jaes0-28086
4. Babaytsev AV, Rabinskiy LN (2019) Design calculation technique for thick-walled composite constructions operating under high-speed loading. Per Tche Quim 16(33):480–489
5. Dobryanskiy VN, Rabinskiy LN, Tushavina OV (2019) Experimental finding of fracture toughness characteristics and theoretical modeling of crack propagation processes in carbon fiber samples under conditions of additive production. Per Tche Quim 16(33):325–336
6. Solyaev Y, Babaytsev A (2021) Direct observation of plastic shear strain concentration in the thick GLARE laminates under bending loading. Compos Part B Eng 224:109145. https://doi.org/10.1016/j.compositesb.2021.109145

7. Afanasev VA, Nikitin PV, Tushavina OV (2019) Behavior of titanium alloys in aerodynamic heating of hypersonic airplanes. Russ Eng Res 39(1):25–30. https://doi.org/10.3103/S1068798X1901012X

8. Amosov AG (2021) Special software application for antenna modelling in mechanical engineering. J Phys Conf Ser 1889(4):042031. https://doi.org/10.1088/1742-6596/1889/4/042031

9. Amosov AG (2021) Curvilinear trajectory of track machines. AIP Conf Proc 2402(1):020022. https://doi.org/10.1063/5.0071513

10. Kuznetsova EL, Rabinskiy LN (2019) Heat transfer in nonlinear anisotropic growing bodies based on analytical solution. Asia Life Sci 2(21):837–846

11. Nicholas T (1999) Critical issues in high cycle fatigue. Int J Fat 21:221–231

12. Shanyavskiy AA (2014) Very-high-cycle-fatigue of in-service air-engine blades, compressor and turbine. Sci China Phys Mech Astr 57(1):19–29

13. Kuznetsova EL, Rabinskiy LN (2019) Modeling the effects of buckling arising in production of thin-walled parts using selective laser melting (SLM) technology. Asia Life Sci 1(21):601–611

14. Hein TZ, Babaytsev AV, Ripetskiy AV (2022) Effect of build atmosphere on the surface roughness of AlSi10Mg samples produced by selective laser melting. Nanlinear Technol Int J 13(1):1–9. https://doi.org/10.1615/NanoSciTechnolIntJ.2021038846

15. Dobryanskiy VN, Rabinskiy LN, Tushavina OV (2019) Validation of methodology for modeling effects of loss of stability in thin-walled parts manufactured using SLM technology. Per Tche Quim 16(33):650–656

16. Babaytsev AV, Orekhov AA, Rabinskiy LN (2020) Properties and microstructure of AlSi10Mg samples obtained by selective laser melting. Nanlinear Technol 11(3):213–222. https://doi.org/10.1615/NanoSciTechnolIntJ.2020034207

17. Shanyavskiy AA, Nikitin AD, Belousov GG (2015) Very-high-cycle-fatigue regime of in-service titanium blades subjected to multiaxial loading during aircraft accessory power plant operations. In: proceedings of the tenth international conference on multiaxial fatigue fracture, p 8.

18. Sakai T (2009) Review and prospects for current studies on very high cycle fatigue of metallic materials for machine structural use. J Solid Mech Mater Eng 3(3):425–439

19. Antolovich SD, Mughrabi H (2016) In memoriam Claude Bathias 1938–2015. Int J Fat 93:215

20. Spriestersbach D, Grad P, Kerscher E (2014) Crack initiation mechanisms and threshold values of very high cycle fatigue failure of high strength steels. Proc Eng 74:84–91

21. Jeddi D, Palin-Luc T (2018) A review about the effects of structural and operational factors on the gigacycle fatigue of steels. Fat Fract Eng Mater Struct 41(5):969–990

22. Bathias C (2006) Piezoelectric fatigue testing machines and devices. Int J Fat 28(11):1438–1445

23. Bathias C, Drouillac L, Le Francois P (2001) How and why the fatigue S–N curve does not approach a horizontal asymptote. Int J Fat 23:143–151

24. Ravi Chandran KS, Jha SK (2005) Duality of the S–N fatigue curve caused by competing failure modes in a titanium alloy and the role of Poisson defect statistics. Acta Mat 53(7):1867–1881

25. Nikitin A, Palin-Luc T, Shanyavskiy A, Bathias C (2016) Comparison of crack paths in a forged and extruded aeronautical titanium alloy loaded in torsion in the gigacycle fatigue regime. Eng Fract Mech 167:259–272

26. Jha SK, Ravi Chandran KS (2003) An unusual fatigue phenomenon: duality of the S–N fatigue curve in the b-titanium alloy Ti–10V–2Fe–3Al. Scripta Mat 48(8):1207–1212

27. Burago NG, Nikitin AD, Nikitin IS, Yushkovsky PA (2016) Stationary vibrations and fatigue failure of compressor disks of variable thickness. Proc Struct Int 2:1109–1116

28. Nikitin IS, Burago NG, Nikitin AD, Yakushev VL (2017) Determination of the critical plane and assessment of fatigue life under various modes of cyclic loading. Bull Perm Nat Res Pol Un Mech 4:238–252

29. Nikitin A, Palin-Luc T, Shanyavskiy A (2016) Crack initiation in VHCF regime on forged titanium alloy under tensile and torsion loading modes. Int J Fat 93:318–325

30. Bandara CS, Siriwardane SC, Dissanayake UI, Dissanayake R (2013) Fatigue strength prediction formulae for steels and alloys in the Gigacycle regime. Int J Mater Mech Man 1(3):256–260

31. Nikitin A, Bathias C, Palin-Luc T, Shanyavskiy A (2015) Crack path in aeronautical titanium alloy under ultrasonic torsion loading. Fratt ed Int Strutt 35:213–222

32. Nikitin AD, Shanyavskii AA, Beklemishev NN, Porokhov VV, Barsegyan OS (2018) Effect of microstructural features of titanium alloys on fatigue properties and mechanism of crack nucleation in region of very high cycle fatigue. Inorg Mat Appl Res 9(4):612–619

33. Bannikov MV, Naimark OB, Oborin VA (2016) Experimental investigation of crack initiation and propagation in high-and gigacycle fatigue in titanium alloys by study of morphology of fracture. Fratt Int Strutt 10(35):51–56

34. Kuznetsova EL, Rabinskiy LN (2019) Numerical modeling and software for determining the static and linkage parameters of growing bodies in the process of non-stationary additive heat and mass transfer. Per Tche Quim 16(33):472–479

35. Astapov A, Rabinskiy L, Tushavina O (2021) Oxidation resistance of a Si–TiSi$_2$–MoSi$_2$–TiB$_2$–CaSi$_2$ coating on a Cf/C–SiC substrate in high-speed high-enthalpy air plasma flows. Nanomat 11(10):2637

36. Astapov AN, Zhavoronok SI, Kurbatov AS, Rabinskiy LN, Tushavina OV (2021) Main problems in the creation of thermal-protection systems based on structurally heterogeneous materials and the methods of their solution. High Temp 59(2):346–372

37. Sha M, Rabinskiy L, Utkin YA (2021) Development of manufacturing technology of nozzles from composite materials during radiation cooling. Int J Adv Sci Eng Inf Technol 11(6):2299–2304

38. Bulychev NA, Rabinskiy LN, Tushavina OV (2020) Effect of intense mechanical vibration of ultrasonic frequency on thermal unstable low-temperature plasma. Nan Techn 11(1):15–21

39. Bathias C, Paris P (2004) Gigacycle fatigue in mechanical practice. Dekker, New York

40. Manson SS (1954) National advisory committee on aerospace technical note 2933. National Advisory Committee, Cleveland.

41. Wu T, Ni J, Bathias C (1994) An automatic ultrasonic fatigue testing system for studying low crack growth at room and high temperatures. In: automation in fatigue and fracture: testing and analysis. ASTM International, West Conshohocken pp 10–21

42. Nikitin A, Bathias C, Palin-Luc T (2015) A new piezoelectric fatigue testing machine in pure torsion for ultrasonic gigacycle fatigue tests: application to forged and extruded titanium alloys. Fat Fract Eng Mater Struct 38(11):1294–1304

43. ASTM E466–15 (2007) Standard practice for conducting force controlled constant amplitude axial fatigue tests of metallic materials. ASTM International: West Conshohocken pp 1

44. Shanyavskiy A (2016) Scales of metal fatigue failures and mechanisms for origin of subsurface fracture formation. Sol State Phen 258:249–254

45. Bache MR (1999) Processing titanium alloys for optimum fatigue performance. Int J Fat 21:105–111

46. Pan X, Xu S, Qian G, Nikitin A, Shanyavskiy A, Palin-Luc T, Hong Y (2020) The mechanism of internal fatigue-crack initiation and

early growth in a titanium alloy with lamellar and equiaxed microstructure. Mat Sci and Eng: A 798:140110

47. Everaerts J, Verlinden B, Wevers M (2017) Investigation of fatigue crack initiation facets in Ti-6Al-4V using focused ion beam milling and electron backscatter diffraction. J Microsc 267(1):57–69

48. Sakai T, Ochi Y (2004) Very high cycle fatigue. In: proceedings of the third international conference on very high cycle fatigue (VHCF-3), pp 16–19. Ritsumeikan University: Kusatsu, Japan